ULTRASONIC PHYSICAL MECHANISMS AND CHEMICAL EFFECTS

The irradiation of liquids with high-intensity ultrasound causes chemical reactions to occur (1–6), often with the emis-

sion of light (5–10). Acoustic cavitation (the formation, growth, and implosive collapse of bubbles in liquids irradiated with sound) is the phenomenon responsible for sonochemistry and sonoluminescence. During cavitation, the collapse of bubbles produces intense local heating and high pressures, with very short lifetimes. In clouds of cavitating bubbles, these hot-spots have equivalent temperatures of roughly 5000 K, pressures of about 1000 atmospheres, and heating and cooling rates above 10^{10} K/s (11,12). In single-bubble cavitation, conditions may be even more extreme. Cavitation, then, can create extreme physical and chemical conditions in otherwise cold liquids.

If liquids containing solids are irradiated with ultrasound, related phenomena can occur. Near an extended solid surface, cavity collapse becomes nonspherical, which drives high-speed jets of liquid into the solid surface (5,13). These jets and associated shock waves can cause substantial surface damage and expose fresh, highly heated surfaces. In addition, high-velocity interparticle collisions will occur during ultrasonic irradiation of liquid-powder suspensions through cavitation and the shockwaves it creates in such slurries (14). The resultant collisions are capable of inducing dramatic changes in surface morphology, composition, and reactivity (15,16).

There are two general classes of sonochemical reactions, based on the nature of the cavitation event: (1) homogeneous sonochemistry of liquids, (2) heterogeneous sonochemistry of liquid-liquid or liquid-solid systems, and sonocatalysis (which overlaps the first two) (17,18). In some cases, ultrasonic irradiation can increase reactivity by nearly a millionfold. Because cavitation can only occur in liquids, chemical reactions are not generally seen in the ultrasonic irradiation of solids or solid-gas systems (with the exception of trapped liquids within a solid matrix, which can cavitate).

Sonoluminescence may generally be considered a special case of homogeneous sonochemistry; however, recent discoveries in this field, especially from the groups of Crum and Putterman, have heightened interest in the phenomenon in and of itself (7,8). Under conditions where an isolated, single bubble undergoes cavitation, recent studies on the duration of the sonoluminescence flash suggest that under certain conditions a shock wave may be created within the collapsing bubble, with the capacity to generate truly enormous temperatures and pressures within the gas.

ACOUSTIC CAVITATION

Ultrasound spans the frequencies of roughly 15 kHz to 1 GHz. With typical sound velocities in liquids of ≈1500 m/s, acoustic wavelengths range from roughly 10 cm to 10^{-4} cm. These are not molecular dimensions. Consequently, the chemical effects of ultrasound do not arise from a direct interaction with molecular species: no direct coupling of the acoustic field on a molecular level is responsible for sonochemistry or sonoluminescence. Instead, sonochemistry and sonoluminescence derive principally from acoustic cavitation (5), which serves as an effective means of concentrating the diffuse energy of sound. Compression of a gas generates heat. When the compression of bubbles occurs during cavitation, it is more rapid than thermal transport and consequently generates a short-lived, localized hot-spot. (One may consider a convergent shock wave as the limiting case of such compressional heating.) There is a general consensus that this hot-spot is the source of homogeneous sonochemistry. Rayleigh's early descriptions of a mathematical model for the collapse of cavities in incompressible liquids predicted enormous local temperatures and pressures (19). Ten years later, Richards and Loomis reported the first chemical and biological effects of ultrasound (20). Alternative mechanisms involving electrical microdischarge have been occasionally proposed, but remain only a minority viewpoint.

If a moderately intense acoustic field (greater than ≈0.5 MPa) is applied to a liquid, the liquid can fail during the expansion (i.e., tensile or negative pressure) portion of the sound field; weak sites within the liquid (e.g., preexisting gas pockets, called "cavitation nuclei") are caused to rapidly grow, thereby producing vapor and gas-filled cavities (i.e., bubbles). These bubbles continue to grow during the negative-pressure portion of the sound field, until the sound field pressure turns positive. The resulting inertial implosion of the bubbles (now mostly filled with vapor and thus unable to provide stiffness) can be extremely violent, leading to an enormous concentration of energy within the small residual volume of the collapsed bubble (Fig. 1). This violent cavitation event has been termed "transient cavitation." A normal consequence of this unstable growth and subsequent collapse is that the cavitation bubble itself is destroyed. Gas-filled remnants from the collapse, however, may serve as nucleation sites for subsequent cycles.

For the generally accepted hot-spot theory, the potential energy of the bubble increases as it expands to maximum size, and this energy is then spatially and temporally concentrated into a heated gas core as the bubble implodes. The oscillations of a gas bubble driven by an acoustic field are generally described by the "Rayleigh–Plesset" equation; one form of which, called the Gilmore equation (5), can be expressed as a second-order nonlinear differential equation given as

$$R\left(1-\frac{U}{C}\right)\frac{d^2R}{dt^2}+\frac{3}{2}\left(1-\frac{U}{3C}\right)\left(\frac{dR}{dt}\right)^2 - \left(1+\frac{U}{C}\right)H-\frac{R}{C}\left(1-\frac{U}{C}\right)\frac{dH}{dt}=0 \quad (1)$$

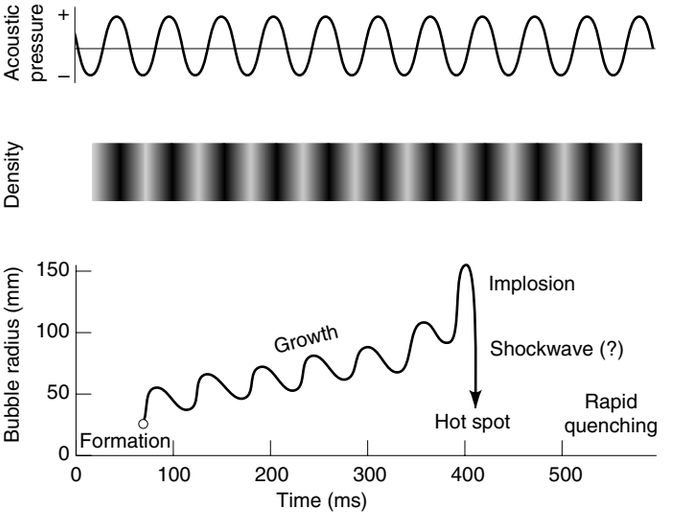

Figure 1. Transient acoustic cavitation: the origin of sonochemistry and sonoluminescence.

The radius and velocity of the bubble wall are given by R and U, respectively. The values for H, the enthalpy at the bubble wall, and C, the local sound speed, may be expressed as follows, using the Tait equation of state for the liquid:

$$H = \frac{n}{n-1}\frac{A^{1/n}}{\rho_o}\left\{[P(R)+B]^{n-1/n} - [P_\infty(t)+B]^{n-1/n}\right\} \qquad (2)$$

and

$$C = [c_o^2 + (n-1)H]^{1/2} \qquad (3)$$

The linear speed of sound in the liquid is c_0. A, B, and n are constants which should be set to the appropriate values (for water these values are A = 3001 atm., $B = A-1$, and n = 7). The term $P_\infty(t)$ is the pressure far from the bubble, and includes the ambient pressure plus an appropriate acoustic forcing function. The pressure at the bubble wall (assuming an ideal gas obeying the polytropic law) is given by

$$P(R) = \left(P_o + \frac{2\sigma}{R_0}\right)\left(\frac{R_o}{R}\right)^{3\gamma} - \frac{2\sigma}{R} - \frac{4\mu U}{R} \qquad (4)$$

where the initial radius of the bubble at time zero is R_0. The ambient pressure of the liquid is P_0, the surface tension σ, the shear viscosity μ, and the polytropic exponent γ.

The validity of the Gilmore equation to compute the behavior of a single, isolated cavitating bubble has been experimentally confirmed. For example, using a light-scattering technique, various researchers have obtained measurements of the radius-time curve for single cavitating bubbles (Fig. 2), simultaneous with optical emission from sonoluminescence. The single-bubble sonoluminescent emission is seen as the sharp spike, appearing at the final stages of bubble collapse. Note that these emissions occur at the point of minimum bubble size, and that the general shape of the theoretical radius-time curve is reproduced (21,22).

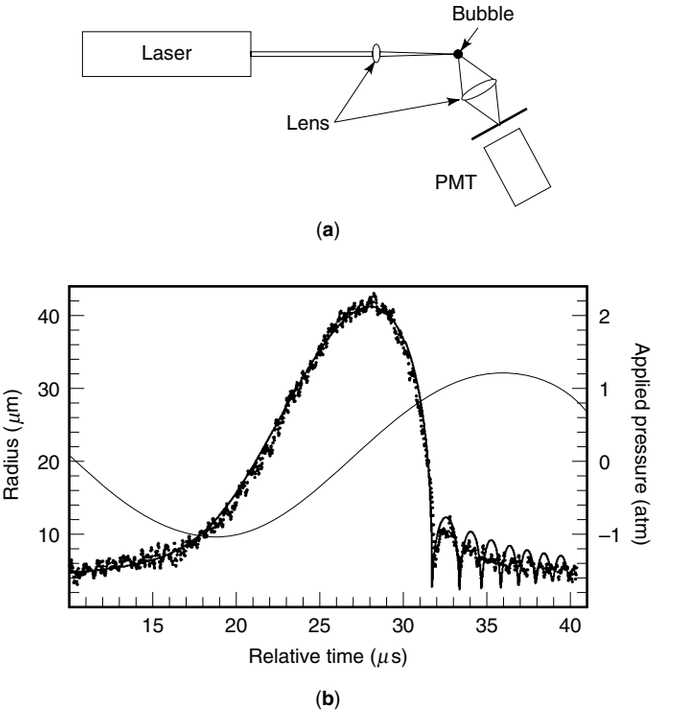

Figure 2. Radius-time curves for single cavitating bubbles. (a) A 30 mW HeNe laser is used as a light source to scatter light off the bubble. The scattered light is collected with a lens and focused onto a photomultiplier tube (PMT). The intensity of the scattered light is determined by Mie scattering theory; however, if the collection optics covers a large solid angle, and the bubble is greater than a few microns, then in this geometrical optics limit, the intensity is proportional to the square of the bubble radius. (b) The collected scattered light is fit to the Gilmore equation assuming the geometrical optics limit, in this case for R_0 = 5.25 μm, P_a = 1.40 atm, and R_{max} = 35 μm, f = 33.8 kHz. The rest of the variables are for water at room temperature.

TWO-SITE MODEL OF SONOCHEMICAL REACTIVITY

The complex environment that is present in a cavitation field, in which hundreds or thousands of cavitation bubbles interact during their transient cavitation behavior, precludes conventional measurement of the conditions generated during bubble collapse. Chemical reactions themselves, however, can be used to probe reaction conditions. The effective temperature realized by the collapse of clouds of cavitating bubbles can be determined by the use of competing unimolecular reactions whose rate dependencies on temperature have already been measured. This technique of "comparative-rate chemical thermometry" was used by Suslick, Hammerton, and Cline to first determine the effective temperature reached during cavity collapse (11). The sonochemical ligand substitutions of volatile metal carbonyls were used as these comparative rate probes. These kinetic studies revealed that there were, in fact, *two* sonochemical reaction sites: the first (and dominant site) is the bubble's interior gas-phase, while the second is an *initially* liquid phase. The latter corresponds either to heating of a shell of liquid around the collapsing bubble or to droplets of liquid ejected into the hot-spot by surface wave distortions of the collapsing bubble, as shown schematically in Fig. 3.

In addition, for both sites an effective local temperature was determined by combining the relative sonochemical reaction rates with the known temperature behavior of these reactions. The effective temperature of these hot-spots was measured at ≈5200 K in the gas-phase reaction zone and ≈1900 K in the initially liquid zone (11). Of course, the comparative rate data represent only a composite temperature: during the collapse, the temperature has a highly dynamic profile, as well as a spatial temperature gradient. This two-site model has been confirmed with other reactions (23) and alternative measurements of local temperatures by multibubble sonoluminescence are consistent (12), as discussed later.

MICROJET FORMATION DURING CAVITATION AT LIQUID–SOLID INTERFACES

Very different phenomena occur for cavitation near extended liquid–solid interfaces. There are two proposed mechanisms for the effects of cavitation near surfaces: (1) microjet impact and (2) shockwave damage. Whenever a cavitation bubble is produced near a boundary, the asymmetry of the liquid particle motion during cavity collapse induces a deformation in the

cavity (5). The potential energy of the expanded bubble is converted into kinetic energy of a liquid jet that extends through the bubble's interior and penetrates the opposite bubble wall. Because most of the available energy is transferred to the accelerating jet, rather than the bubble wall itself, this jet can reach velocities of hundreds of meters per second. Because of the induced asymmetry, the jet often impacts the local boundary and can deposit enormous energy densities at the site of impact, especially for larger bubbles (i.e., lower frequency). Figure 4 shows a photograph of a jet developed in a collapsing cavity. The second mechanism of cavitation-induced surface damage invokes shockwaves created by cavity collapse in the liquid. The impingement of microjets and shockwaves on the surface creates the localized erosion responsible for ultrasonic cleaning and many of the sonochemical effects on heterogeneous reactions. The erosion of metals by cavitation generates newly exposed, highly heated surfaces. Such energy concentration can result in severe damage to the boundary surface; this is less true at higher (MHz) frequencies, simply because the cavitation bubbles are much smaller. This explains the increasing interest in high-frequency ultrasonic cleaning for microelectronics (which has been given unfortunate marketing label "megasonics").

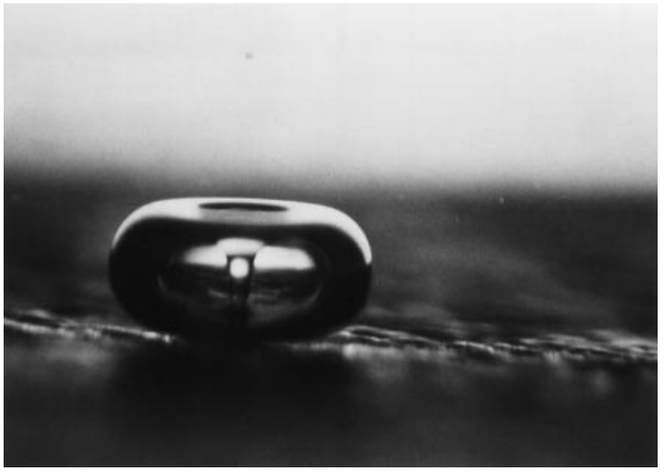

Figure 4. Photograph of liquid jet produced during collapse of a cavitation bubble near a solid surface. The width of the bubble is about 1 mm. Reproduced with permission (13).

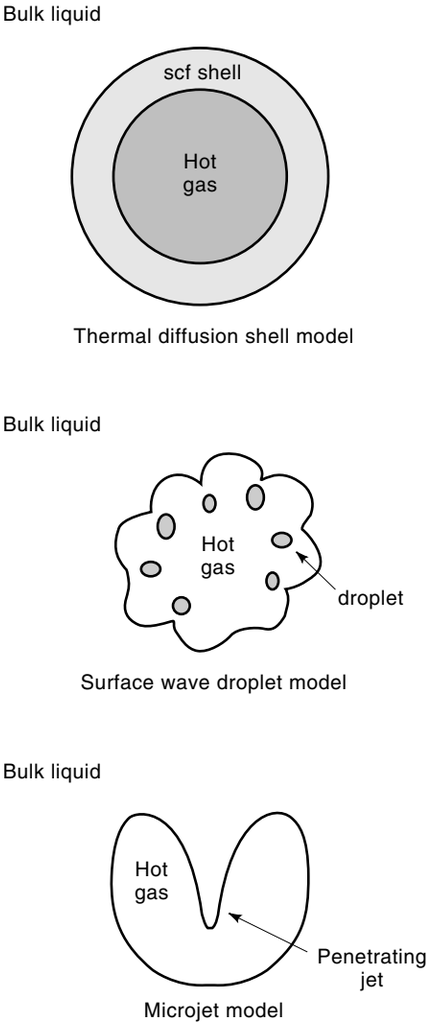

Figure 3. Two-site models of the sonochemical reactions sites.

In order to induce substantial distortions during bubble collapse, the solid surface must be several times larger than the resonance bubble size: at ≈20 kHz, jet formation becomes important if the solid particles are larger than ≈200 μm. For smaller particles, the shockwaves created by homogeneous cavitation can create high-velocity interparticle collisions (14). Suslick and coworkers have found that the turbulent flow and shockwaves produced by intense ultrasound can drive metal particles together at sufficiently high speeds to induce effective melting in direct collisions (Fig. 5) and the abrasion of surface crystallites in glancing impacts (Fig. 6). A series of transition metal powders were used to probe the maximum temperatures and speeds reached during interparticle collisions. Using the irradiation of Cr, Mo, and W powders in decane at 20 kHz and 50 W/cm^2, agglomeration and essentially a localized melting occurs for the first two metals, but not the third. On the basis of the melting points of these metals, the effective transient temperature reached at the point of impact during interparticle collisions is roughly 3000°C (which is unrelated to the temperature inside the hotspot of a collapsing bubble). From the volume of the melted region of impact, the amount of energy generated during collision was determined. From this, a lower estimate of the velocity of impact is roughly one-half the speed of sound, in agreement with expected particle velocities from cavitation-induced shockwaves in the liquid.

SONOLUMINESCENCE

Types of Sonoluminescence

Ultrasonic irradiation of liquids can also produce light, termed "sonoluminescence," as first observed from water in 1934 by Frenzel and Schultes (24). As with sonochemistry, sonoluminescence derives from acoustic cavitation. It is now generally thought that there are two classes of sonoluminescence: multiple-bubble sonoluminescence (MBSL) and single-bubble sonoluminescence (SBSL) (2,7,10,21,25). Since cavita-

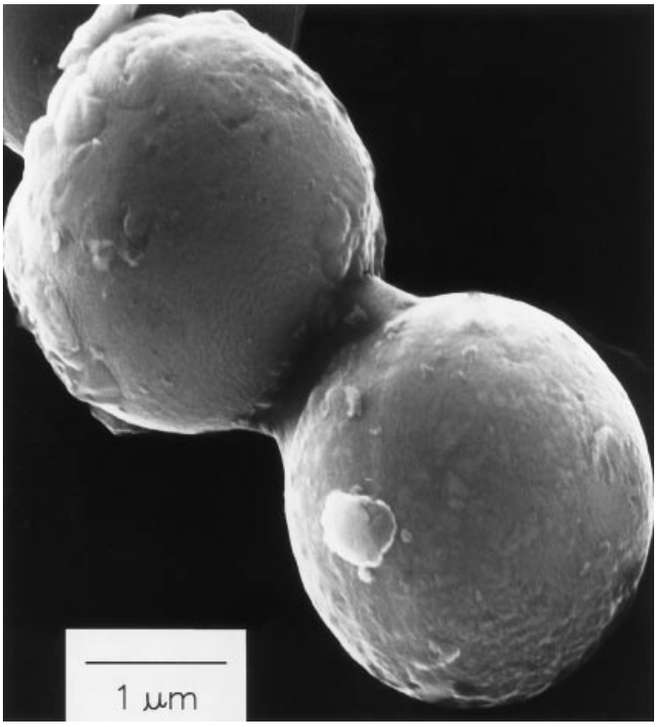

Figure 5. Scanning electron micrograph of 5 μm diameter Zn powder. Neck formation from localized melting is caused by high-velocity interparticle collisions. Similar micrographs and elemental composition maps (by Auger electron spectroscopy) of mixed metal collisions have also been made. Reproduced with permission (14).

tion is a nucleated process and liquids generally contain large numbers of particulates that serve as nuclei, the "cavitation field" generated by a propagating or standing acoustic wave typically consists of very large numbers of interacting bubbles, distributed over an extended region of the liquid. Such cavitation can be sufficiently intense to produce multiple-bubble sonoluminescence (MBSL).

For rather specialized but easily obtainable conditions, it was recently discovered that a single, stable gas bubble can be forced into such large amplitude pulsations that it produces sonoluminescence emission on each (and every) acoustic cycle (26,27). This phenomenon is called single-bubble sonoluminescence (SBSL), and has received considerable recent attention (7,8,28,29). Under the appropriate conditions, the acoustic force on a bubble can be used to balance against its buoyancy, holding the bubble stable in the liquid by acoustic levitation. This permits examination of the dynamic characteristics of a single cavitating bubble in considerable detail, from both a theoretical and an experimental perspective. Such a bubble is typically quite small, compared with an acoustic wavelength (e.g., at 20 kHz, the resonance size is approximately 150 μm).

Multiple-Bubble Sonoluminescence

The sonoluminescence of aqueous solutions has been studied extensively over the past thirty years. The spectrum of MBSL in water consists of a peak at 310 nm and a broad continuum throughout the visible region. An intensive study of aqueous MBSL was conducted by Verrall and Sehgal (9) and later by Didenko (30). The emission at 310 nm is from excited-state $OH^{\bullet}$, but the continuum is difficult to interpret. MBSL from aqueous and alcohol solutions of many metal salts have been reported and are characterized by emission from metal atom excited states (31).

Flint and Suslick reported the first MBSL spectra of organic liquids (32). With various hydrocarbons, the observed emission is from excited states of C_2 ($d^3\Pi_g$–$a^3\Pi_u$, the Swan lines), the same emission seen in flames. Furthermore, the ultrasonic irradiation of alkanes in the presence of N_2 (or NH_3 or amines) gives emission from CN-excited states, but not from N_2-excited states. Emission from N_2-excited states would have been expected if the MBSL originated from microdischarge, whereas CN emission is typically observed from thermal sources. When oxygen is present, emission from excited states of CO_2, $CH^{\cdot}$, and $OH^{\cdot}$, is observed, again similar to flame emission.

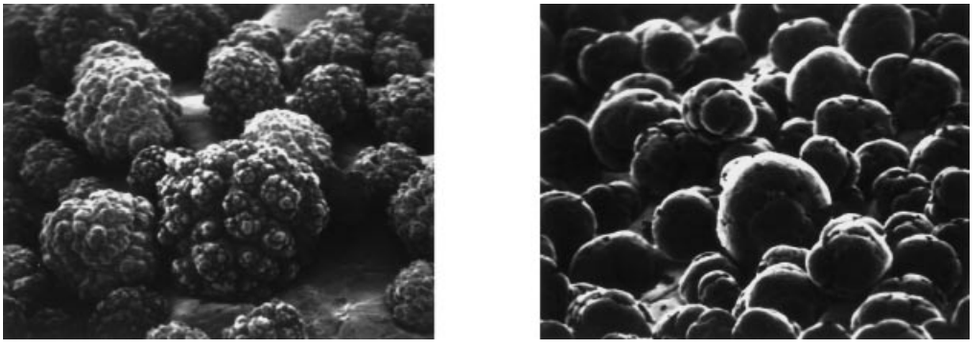

Figure 6. The effect of ultrasonic irradiation on the surface morphology and particle size of Ni powder. Initial particle diameters before ultrasound were ≈160 μm; after ultrasound, ≈80 μm. High-velocity interparticle collisions caused by ultrasonic irradiation of slurries are responsible for the smoothing and removal of passivating oxide coating. Reproduced with permission (15).

For both aqueous and nonaqueous liquids, the emission spectra from MBSL suggests that the principal source of light emission is from chemical reactions involving high-energy species formed during cavitation by bubble collapse. MBSL is principally a form of chemiluminescence, just as flame emission is.

Single-Bubble Sonoluminescence

At the time of this writing, our understanding of SBSL remains in a state of flux. New discoveries are being announced every few months, and theoretical interpretations of the experimental findings continue to be refined. It is not yet possible to provide a definitive mechanism for the light emission process, although the most favored model involves compressional heating (possibly with a convergent shockwave) of the bubble contents, similar to MBSL. The spectra of MBSL and SBSL, however, show some dramatic differences. While MBSL is generally dominated by atomic and molecular emission lines, SBSL is an essentially featureless emission that increases with decreasing wavelength. For example, an aqueous solution of NaCl shows evidence of excited states of both $OH^{\cdot}$ and Na in the MBSL spectrum; however, the SBSL spectrum of an identical solution shows no evidence of either of these peaks (Fig. 7) (25). Similarly, the MBSL spectrum falls off sharply at low wavelengths, while the SBSL spectrum continues to rise, at least for bubbles containing most noble gases (29). Nevertheless, the commonality of cause (acoustic cavitation) and effect (light emission) suggests some association in the underlying physics of sonoluminescence for both MBSL and SBSL. The most plausible explanation for the differences between MBSL and SBSL is simply the degree of compression and the extent of consequent local heating. In SBSL, the bubble collapse is much more spherical than is likely in the complex acoustics of a bubble cloud. As a consequence, perhaps with the assistance of a convergent shock wave, the effective temperature reached in single-bubble cavitation is probably sufficiently high to induce significant ionization and plasma formation. Under these circumstances, SBSL will be dominated by featureless bremsstrahlung emission, rather than bands from atomic or molecular emission as in MBSL.

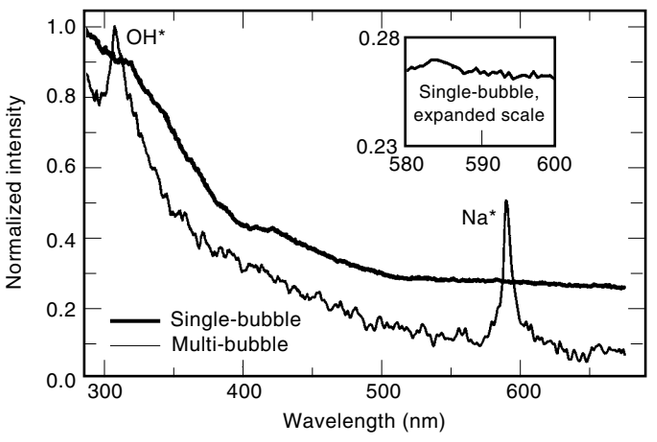

Figure 7. A comparison of sonoluminescence spectra of an aqueous solution of sodium chloride from SBSL and MBSL shows some dramatic differences, and some interesting similarities. The tell-tale sodium line is easily evident with MBSL, but no such line appears in the SBSL spectrum. Also, the excited state hydroxyl radical emission band at 310 nm is observed in MBSL, but not in SBSL. Interestingly, the continuum of both systems is seen to increase into the near UV.

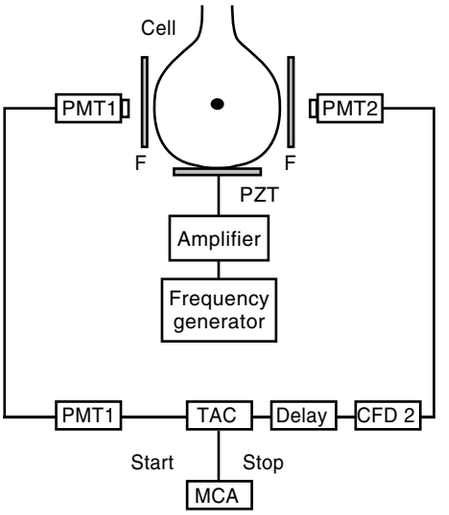

Figure 8. A single-bubble sonoluminescence apparatus. A piezoelectric transducer (PZT), mounted to a water-filled levitation cell, is driven by a frequency generator/power amplifier combination. The frequency generator drives the PZT at the appropriate frequency to generate a standing acoustic wave profile within the levitation cell. The power amplifier adds gain to the signal so that the pressure amplitude at the pressure antinode is about 1 atm. A transducer matchbox is used for impedance-matching purposes. For experiments to measure the pulse duration from single-bubble sonoluminescence, a time-correlated single photon counting method works so long as the bubble remains stable and light emission occurs in a synchronous fashion. Light is collected by two microchannel plate photomultiplier tubes (MCPPMTs) after passing through bandpass filters. The filters are used to ensure that similar-energy photons are being measured. A constant fraction discriminator (CFD) is used to precisely time the events, while a time-to-amplitude converter (TAC) measures the time difference between the two pulses. The output of the TAC is fed into a multichannel analyzer (MCA), which displays a histogram of the time difference between the received signals.

Figure 8 illustrates a typical experimental setup for generating SBSL. A piezoelectric, mounted to a water-filled acoustic levitation cell, is driven to set up a standing wave within the water. The drive frequency depends on the size and geometry of the levitation cell (which can be spherical, cylindrical, or even rectangular). The water is typically degassed to about 10% of saturation. A bubble is introduced by injecting air through a syringe into the water. The large bubbles rise to the surface, while the small bubbles are attracted to pressure antinodes. The final size of the remaining bubble at the antinode depends on gas diffusion steady-state conditions and instabilities present: if the bubble is too small, gas will transport into the bubble; if the bubble is too large, small microbubbles will be ejected from the main bubble. In this manner, the final bubble comes into a diffusive steady state.

Once the bubble is positioned at the pressure antinode, the drive pressure amplitude is increased until sonoluminescence is observed. Figure 9 illustrates the various regions in the drive pressure parameter space that the bubble experiences. At low drive pressures, the bubble experiences small amplitude linear oscillations. As the drive amplitude increases,

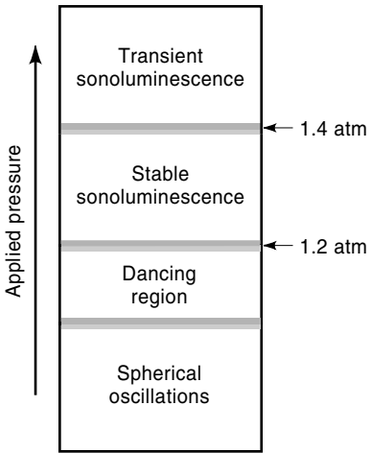

Figure 9. The various regions in the drive pressure parameter space are illustrated here. Stable single-bubble sonoluminescence is observed between about 1.2 atm and 1.4 atm. The regions are separated by thresholds that are not precisely defined.

nonlinear oscillations develop, as well as instabilities; the bubble is seen to "dance" around, ejecting microbubbles, and remains in an unstable state. If the drive pressure is increased further, beyond about 1.2 atm, the bubble is observed to seemingly lock into a mode that corresponds to sonoluminescence. At this time, there is not yet a consensus as to the mechanism for this behavior. Further increases in intensity result in higher light output from the bubble. Finally, at around 1.4 atm, the bubble self-destructs, due to parametric or other instabilities.

The radial motion of the bubble was illustrated in Fig. 2. During the main collapse of the bubble, the interior heats up and at the final stages of collapse, light is emitted. With SBSL, the light-emission process may occur each and every acoustic cycle, with a synchronicity better than 1 ppb; for instance, in a 20 kHz sound field (with a period of 50 μs), the light emission can have a jitter of less than 50 ps.

One intriguing aspect of SBSL is the extremely short duration of the sonoluminescence flash. The hydrodynamic models of adiabatic collapse of a single bubble suggest that the temperature of the gas within the bubble should remain at elevated temperatures for times lasting tens of nanoseconds (33). However, the measured pulse duration of the light flash has been shown to be below 200 ps (34), and possibly less than 50 ps in some cases (35,36). Figure 8 also shows an experiment designed to measure the short pulse duration from SBSL. Due to the low levels of light output from a sonoluminescing bubble, one cannot simply use picosecond-response photodiodes. More sophisticated experiments are required. In this case, time-correlated single photon counting is used to measure the pulse duration. Since the experiment measures the time difference between two photons occurring during the same flash, this measurement produces an autocorrelation of the pulse. Due to the complex and transient nature of cavitation fields, one cannot employ such averaging techniques to MBSL. The most recent studies of MBSL have shown that for aqueous systems involving air and noble gases, the pulse width is also extremely short, much less than 1 ns (37).

Recently, Lohse, Brenner, and Hilgenfeldt have proposed a new hypothesis that may dramatically affect the interpretations of comparisons made between MBSL and SBSL (38,39). For MBSL, it is generally accepted that a particular bubble in the cavitation field only lasts for a few acoustic cycles before being destroyed, and therefore its contents represent the equilibrium vapor pressures of the solution and its dissolved gases. In contrast, in SBSL, a single bubble can remain stable, emitting light for hours. For air bubbles in water, Lohse and coworkers suggest that nitrogen and oxygen molecules dissociate because of the high temperatures, forming NO_x compounds that dissolve in the surrounding water, leaving behind only the nonreactive argon inside the bubble. Thus, even though argon represents only a small fraction of the air concentration dissolved in water, the SBSL bubble acts as a chemical reaction chamber that rectifies argon over thousands of acoustic cycles, until the bubble contents are mostly rarefied argon. Experimental proof for the argon-rectification hypothesis may be difficult to acquire, since there are only around 10^9 molecules in an ambient (5 μm radius) SBSL bubble. However, circumstantial evidence is available (38–40).

Recently, using a femtosecond laser, Weninger and colleagues (41) discovered that near the final stages of single-bubble collapse, the bubble interface appears to be moving at a velocity near mach 4 (relative to the speed of sound at *ambient* conditions). This rapidly moving interface suggests that shock waves within the gas are a likely product of imploding single bubbles. If shock waves do indeed form, exciting possibilities can be inferred about the temperatures that could be attained within the bubble and the physics that might result. Indeed, speculations on the possibilities of inertial confinement (*hot*) fusion have been made (42). Since the bubble is assumed to be spherical, it was expected that the light emissions from the bubble would be isotropic and not have any preferred direction in space. However, there is some evidence that under certain conditions the emission has a dipole pattern (43), suggesting the presence of asymmetrical bubble shapes, and other possibilities (including liquid jets).

Spectroscopic Probes of Cavitation Conditions

Determination of the temperatures reached in cavitating bubbles has remained a difficult experimental problem. As a spectroscopic probe of the cavitation event, MBSL provides a solution. High-resolution MBSL spectra from silicone oil under Ar have been reported and analyzed (12). The observed emission comes from excited states of diatomic carbon (C_2) and has been modeled with synthetic spectra as a function of rotational and vibrational temperatures, as shown in Fig. 10. From comparison of synthetic to observed spectra, the effective cavitation temperature is 5050 $\pm$ 150 K. The excellence of the match between the observed MBSL and the synthetic spectra provides definitive proof that the sonoluminescence event is a thermal chemiluminescence process. The agreement between this spectroscopic determination of the cavitation temperature and that made by comparative rate thermometry of sonochemical reactions (11) is surprisingly close.

The interpretation of the spectroscopy of SBSL is much less clear. At this writing, SBSL has been observed primarily in aqueous fluids, and the spectra obtained are surprisingly featureless. Some very interesting effects are observed when the gas contents of the bubble are changed (29,35). Further-

more, the spectra show practically no evidence of OH emissions, and when He and Ar bubbles are considered, continue to increase in intensity even into the deep ultraviolet. These spectra are reminiscent of black body or bremsstrahlung emission with temperatures *considerably* in excess of 10^4 K and lend some support to the concept of an imploding shock wave (42). Several other alternative explanations for SBSL have been presented, and there exists considerable theoretical activity in this particular aspect of SBSL.

SONOCHEMISTRY

In a fundamental sense, chemistry is the interaction of energy and matter. Chemical reactions require energy in one form or another to proceed: chemistry stops as the temperature approaches absolute zero. One has only limited control, however, over the nature of this interaction. In large part, the properties of a specific energy source determine the course of a chemical reaction. Ultrasonic irradiation differs from traditional energy sources (such as heat, light, or ionizing radiation) in duration, pressure, and energy per molecule. The immense local temperatures and pressures and the extraordinary heating and cooling rates generated by cavitation bubble collapse mean that ultrasound provides an unusual mechanism for generating high-energy chemistry. Like photochemistry, very large amounts of energy are introduced in a short period of time, but it is thermal, not electronic, excitation. As in flash pyrolysis, high thermal temperatures are reached, but the duration is very much shorter (by $>10^4$) and the temperatures are even higher (by five- to tenfold). Similar to shock-tube chemistry or multiphoton infrared laser photolysis, cavitation heating is very short lived, but occurs within condensed phases. Furthermore, sonochemistry has a high-pressure component, which suggests that one might be able to produce on a microscopic scale the same macroscopic conditions of high temperature-pressure "bomb" reactions or explosive shockwave synthesis in solids. Figure 11 presents an interesting comparison of the parameters that control chemical reactivity (time, pressure, and energy) for various forms of chemistry.

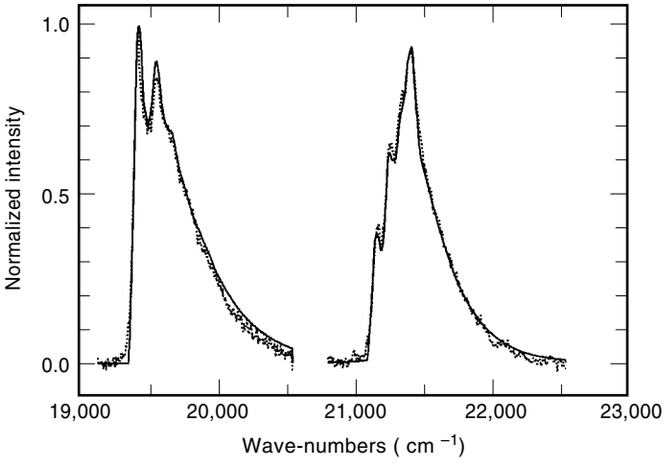

Figure 10. Sonoluminescence of excited state C_2. Emission from the $\Delta\nu = +1$ manifold of the $d^3\Pi_g$–$a^3\Pi_u$ transition (Swan band) of C_2. Dotted line—observed sonoluminescence from polydimethylsiloxane silicone oil under Ar at 0°C; Plain line—best-fit synthetic spectrum, with $T_v = T_r = 4900$ K. Reproduced with permission (12).

The same limitations apply to the control of sonochemical reactions as in any thermal process: the Boltzmann energy distribution means that the energy per individual molecule will vary widely. One does have easy control, however, over the intensity of heating generated by acoustic cavitation using various physical parameters. The origin of these influences is easily understood in terms of the hot-spot mechanism of sonochemistry (1,6). The most important parameters are thermal conductivity of dissolved gases (which can effect the degree of adiabaticity), polyatomic content inside the bubble (which reduces compressional heating), and acoustic pressure. As acoustic pressure is increased, there is a threshold value for nucleation and bubble growth and hence sonochemistry, followed by an increase in sonochemical rates due to increased numbers of effectively cavitating bubbles. At sufficiently high intensities, the cavitation of the liquid near the radiating surface becomes so intense as to produce a shroud of bubbles, diminishing penetration of sound into the liquid and decreasing sonochemical rates. In contrast, frequency appears to be less important, at least within the range where cavitation can occur (a few hertz to a few megahertz), although there have been few detailed studies of its role.

Homogeneous sonochemistry typically is not a very energy efficient process, whereas heterogeneous sonochemistry is several orders of magnitude better. Since ultrasound can be produced with high efficiency from electric power, the primary energy inefficiency is due to the small fraction of the acoustic power actually involved in the cavitation events. This might be significantly improved, however, if a more efficient means of coupling the sound field to generate cavitation can be found.

Experimental Design

A variety of devices have been used for ultrasonic irradiation of solutions. There are three general designs in present use: (1) the ultrasonic cleaning bath, (2) the direct-immersion ultrasonic horn, and (3) the flow reactor. The originating source of the ultrasound is generally a piezoelectric material, usually a lead-zirconate-titanate ceramic (PZT), which is subjected to a high ac voltage with an ultrasonic frequency (typically 15 kHz to 50 kHz). For industrial use, the more robust magnetostrictive metal alloys (usually of Ni) can be used as the core of a solenoid generating an alternating magnetic field with an ultrasonic frequency. The vibrating source is attached to the wall of a cleaning bath, to an amplifying horn, or to the outer surfaces of a flow-through tube or diaphragm.

The ultrasonic cleaning bath is clearly the most accessible source of laboratory ultrasound and has been used successfully for a variety of liquid-solid heterogeneous sonochemical studies. The low intensity available in these devices ($\approx$1 W/cm^2), however, means that even in the case of heterogeneous sonochemistry, an ultrasonic cleaning bath must be viewed as an apparatus of limited capability. The most intense and reliable source of ultrasound generally used in the chemical laboratory is the direct-immersion ultrasonic horn (50 W/cm^2 to 500 W/cm^2), as shown in Fig. 12, which can be used for work under either inert or reactive atmospheres or

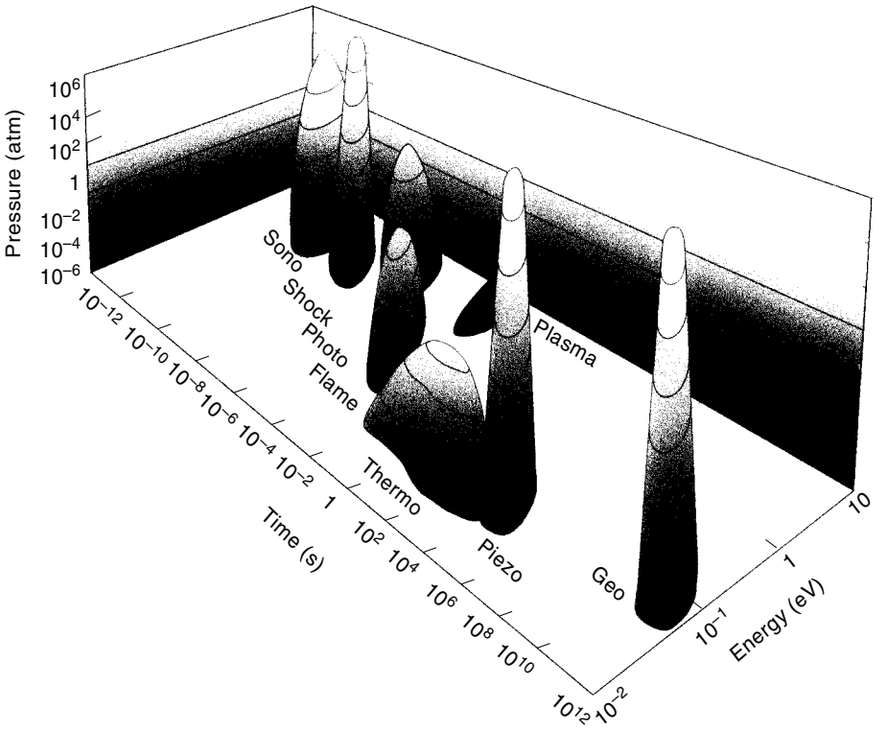

Figure 11. Chemistry—the interaction of energy and matter.

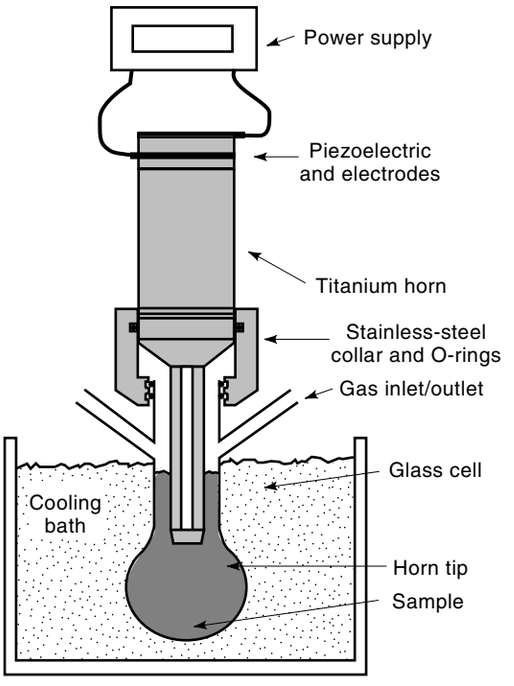

Figure 12. A typical sonochemical apparatus with direct-immersion ultrasonic horn. Ultrasound can be easily introduced into a chemical reaction with good control of temperature and ambient atmosphere. The usual piezoelectric ceramic is PZT, a lead-zirconate-titanate ceramic. Similar designs for sealed stainless-steel cells can operate at pressures above 10 bar.

at moderate pressures (<10 atm). These devices are available from several manufacturers at modest cost. Commercially available flow-through reaction chambers which will attach to these horns allow the processing of multiliter volumes. The acoustic intensities are easily and reproducibly variable; the acoustic frequency is well controlled, albeit fixed (typically at 20 kHz). Since power levels are quite high, countercooling of the reaction solution is essential to provide temperature control. Large-scale ultrasonic generation in flow-through configurations is a well-established technology. Liquid processing rates of 200 L/min are routinely accessible from a variety of modular, in-line designs with acoustic power of ≈20 kW per unit. The industrial uses of these units include (1) degassing of liquids, (2) dispersion of solids into liquids, (3) emulsification of immiscible liquids, and (4) large-scale cell disruption (44,45).

Homogeneous Sonochemistry: Bond Breaking and Radical Formation

The chemical effect of ultrasound on aqueous solutions has been studied for many years. The primary products are H_2 and H_2O_2; there is strong evidence for various high-energy intermediates, including HO_2, $H^{\cdot}$, and $OH^{\cdot}$. The work of Riesz and collaborators used electron paramagnetic resonance with chemical spin-traps to demonstrate definitively the generation of $H^{\cdot}$ and $OH^{\cdot}$ during ultrasonic irradiation, even with clinical sources of ultrasound (46,47). The extensive work in Henglein's laboratory involving aqueous sonochemistry of dissolved gases has established clear analogies to combustion processes (23). As one would expect, the sonolysis of water, which produces both strong reductants and oxidants, is capable of causing secondary oxidation and reduction reactions, as

often observed (48). Most recently there has been strong interest shown in the use of ultrasound for remediation of low levels of organic contamination of water (49,50). The $OH^{\bullet}$ radicals produced from the sonolysis of water are able to attack essentially all organic compounds (including halocarbons, pesticides, and nitroaromatics) and through a series of reactions oxidize them fully. The desirability of sonolysis for such remediation lies in its low maintenance requirements and the low energy efficiency of alternative methods (e.g., ozonolysis, UV photolysis).

In contrast, the ultrasonic irradiation of organic liquids has been less studied. Suslick and coworkers established that virtually all organic liquids will generate free radicals upon ultrasonic irradiation, as long as the total vapor pressure is low enough to allow effective bubble collapse (51). The sonolysis of simple hydrocarbons (e.g., n-alkanes) creates the same kinds of products associated with very-high-temperature pyrolysis. Most of these products (H_2, CH_4, and the smaller 1-alkenes) derive from a well-understood radical chain mechanism.

The sonochemistry of solutes dissolved in organic liquids also remains largely unexplored. The sonochemistry of metal carbonyl compounds is an exception (52). Detailed studies of these systems led to important mechanistic understandings of the nature of sonochemistry. A variety of unusual reactivity patterns has been observed during ultrasonic irradiation, including multiple ligand dissociation, novel metal cluster formation, and the initiation of homogeneous catalysis at low ambient temperature (52).

Applications of Sonochemistry to Materials Synthesis and Catalysis

Of special interest is the recent development of sonochemistry as a synthetic tool for the creation of unusual inorganic materials (16,53). As one example, the recent discovery of a simple sonochemical synthesis of amorphous iron helped settle the longstanding controversy over its magnetic properties (54,55). More generally, ultrasound has proved extremely useful in the synthesis of a wide range of nanostructured materials, including high-surface-area transition metals, alloys, carbides, oxides, and colloids (56,57). Sonochemical decomposition of volatile organometallic precursors in high boiling solvents produces nanostructured materials in various forms with high catalytic activities. Nanometer colloids, nanoporous high-surface-area aggregates, and nanostructured oxide supported catalysts can all be prepared by this general route, as shown schematically in Fig. 13.

Heterogeneous catalysis is extremely important in the chemical and petroleum industries, and the applications of ultrasound to catalysis have been reviewed recently (58). Heterogeneous catalysts often require rare and expensive metals. The use of ultrasound offers some hope of activating less reactive, but also less costly, metals. As one example, ultrasonic irradiation of solutions of $Mo(CO)_6$ produces aggregates of nanometer-sized clusters of face-centered cubic molybdenum carbide. The material was extremely porous with a high surface area and consisted of aggregates of ≈2 nm sized particles. The catalytic properties showed the molybdenum carbide generated by ultrasound is an active and highly selective dehydrogenation catalyst comparable to commercial ultrafine platinum powder. The effects of ultrasound on catalysis can

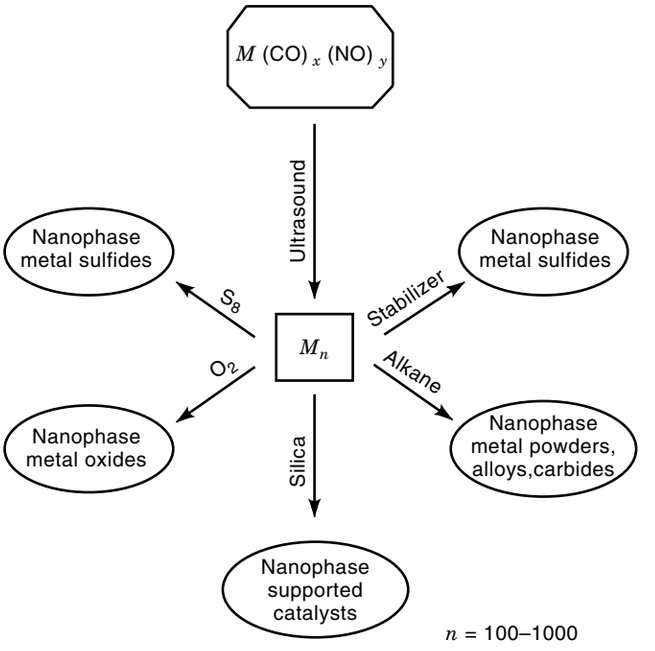

Figure 13. Sonochemical synthesis of various forms of nanostructured materials.

occur in three distinct stages: (1) during the formation of supported catalysts, (2) activation of preformed catalysts, or (3) enhancement of catalytic behavior during a catalytic reaction. In the cases of modest rate increases, it appears likely that the cause is increased effective surface area; this is especially important in the case of catalysts supported on brittle solids. More impressive accelerations, however, have included hydrogenations and hydrosilations by Ni powder, Raney Ni, and Pd or Pt on carbon. For example, the hydrogenation of alkenes by Ni powder is enormously enhanced ($>10^5$-fold) by ultrasonic irradiation. This dramatic increase in catalytic activity is due to the formation of uncontaminated metal surfaces from interparticle collisions caused by cavitation-induced shock waves (58).

Sonochemistry is also proving to have important applications with polymeric materials. Substantial work has been accomplished in the sonochemical initiation of polymerization and in the modification of polymers after synthesis (4). The use of sonolysis to create radicals which function as radical initiators has been well explored. Similarly the use of sonochemically prepared radicals and other reactive species to modify the surface properties of polymers is being developed, particularly by Price. Other effects of ultrasound on long-chain polymers tend to be mechanical cleavage, which produces relatively uniform size distributions of shorter chain lengths.

Another important application has been the sonochemical preparation of biomaterials, most notably protein microspheres (59,60). Using high-intensity ultrasound and simple protein solutions, a remarkably easy method to make both air-filled microbubbles and nonaqueous liquid-filled microcapsules has been developed. These protein microspheres have a wide range of biomedical applications, including their use as echo contrast agents for sonography, magnetic resonance im-

aging contrast enhancement, drug delivery, among others, and have generated a substantial patent estate. The microspheres are stable for months, and being slightly smaller than erythrocytes, can be intravenously injected to pass unimpeded through the circulatory system. The mechanism responsible for microsphere formation is a combination of two acoustic phenomena: emulsification and cavitation. Ultrasonic emulsification creates the microscopic dispersion of the protein solution necessary to form the proteinaceous microspheres. The long life of these microspheres comes from a sonochemical cross-linking of the protein shell. Protein cysteine residues are oxidized during microsphere formation by sonochemically produced superoxide.

Heterogeneous Sonochemistry: Reactions of Solids with Liquids

The use of ultrasound to accelerate chemical reactions in heterogeneous systems has become increasingly widespread. The physical phenomena which are responsible include the creation of emulsions at liquid–liquid interfaces, the generation of cavitational erosion and cleaning at liquid–solid interfaces, the production of shock wave damage and deformation of solid surfaces, the enhancement in surface area from fragmentation of friable solids, and the improvement of mass transport from turbulent mixing and acoustic streaming.

To enhance the reactivity of reactive metals as stoichiometric reagents, ultrasonic irradiation has become an especially routine synthetic technique for many heterogeneous organic and organometallic reactions (15–18), particularly those involving reactive metals, such as Mg, Li, or Zn. This development originated from the early work of Renaud and the more recent breakthroughs of Luche. The effects are quite general and apply to reactive inorganic salts and to main group reagents as well (61). Less work has been done with unreactive metals (e.g., V, Nb, Mo, W), but results here are promising as well (15). Rate enhancements of more than tenfold are common, yields are often substantially improved, and by-products avoided.

The mechanism of the sonochemical rate enhancements in both stoichiometric and catalytic reactions of metals is associated with dramatic changes in morphology of both large extended surfaces and of powders. As discussed earlier, these changes originate from microjet impact on large surfaces and high-velocity interparticle collisions in slurries. Surface composition studies by Auger electron spectroscopy and sputtered neutral mass spectrometry reveal that ultrasonic irradiation effectively removes surface oxide and other contaminating coatings (15). The removal of such passivating coatings can dramatically improve reaction rates. The reactivity of clean metal surfaces also appears to be responsible for the greater tendency for heterogeneous sonochemical reactions to involve single-electron transfer rather than acid–base chemistry.

Applications of ultrasound to electrochemistry have also seen substantial recent progress. Beneficial effects of ultrasound on electroplating and on organic synthetic applications of organic electrochemistry (62) have been known for quite some time. More recent studies have focused on the underlying physical theory of enhanced mass transport near electrode surfaces (63–64). Another important application for sonoelectrochemistry has been developed by Reisse and coworkers for the electroreductive synthesis of submicrometer powders of transition metals (65).

SUMMARY

The phenomenon of acoustic cavitation results in an enormous concentration of energy. If one considers the energy density in an acoustic field that produces cavitation, and that in the collapsed cavitation bubble, there is an amplification factor of over eleven orders of magnitude. The enormous local temperatures and pressures so created result in phenomena such as sonochemistry and sonoluminescence and provide a unique means for fundamental studies of chemistry and physics under extreme conditions. A diverse set of applications of ultrasound to enhancing chemical reactivity has been explored, with important applications in mixed phase synthesis, materials chemistry, and biomedical uses.

BIBLIOGRAPHY

1. K. S. Suslick (ed.), *Ultrasound: Its Chemical, Physical, and Biological Effects,* New York: VCH, 1988.
2. K. S. Suslick, Sonochemistry, *Science,* **247**: 1439, 1990.
3. T. J. Mason (ed.), *Advances in Sonochemistry,* New York: JAI Press, vols. 1–3, 1990, 1991, 1993.
4. G. J. Price (ed.), *Current Trends in Sonochemistry,* Cambridge, UK: R. Soc. Chem., 1992.
5. T. G. Leighton, *The Acoustic Bubble,* London: Academic Press, 1994.
6. K. S. Suslick, Sonochemistry, in *Kirk-Othmer Encyclopedia of Chemical Technology;* 4th ed., New York: Wiley, 1998, vol. 26, pp. 517–541.
7. L. A. Crum, Sonoluminescence, *Phys. Today,* **47** (22): 1994.
8. S. J. Putterman, Sonoluminescence: Sound into light, *Sci. Amer.,* **272** (2): 32–37, 1995.
9. R. E. Verrall and C. Sehgal, Sonoluminescence, in K. S. Suslick (ed.), *Ultrasound: Its Chemical, Physical, and Biological Effects,* New York: VCH, 1988, pp. 227–287.
10. J. D. N. Cheeke, Single-bubble sonoluminescence: Bubble, bubble, toil and trouble, *Can. J. Phys.* **75**: 77–96, 1997.
11. K. S. Suslick, D. A. Hammerton, and R. E. Cline, Jr., The sonochemical hot spot, *J. Amer. Chem. Soc.,* **108**: 5641, 1986.
12. E. B. Flint and K. S. Suslick, The temperature of cavitation, *Science,* **253**: 1397, 1991.
13. L. A. Crum, Acoustic cavitation, *Proc. 1982 Ultrason. Symp.,* **1** (1): 1983.
14. S. J. Doktycz and K. S. Suslick, Inter-particle collisions driven by ultrasound, *Science,* **247**: 1067, 1990.
15. K. S. Suslick and S. J. Doktycz, The effects of ultrasound on solids, *Adv. Sonochem.,* **1**: 197–230, 1990.
16. K. S. Suslick, Applications of ultrasound to materials chemistry, *MRS Bulletin,* **20** (29): 1995.
17. J. L. Luche, Sonochemical activation in organic synthesis, *Comptes Rendus Serie IIB* : 323, 203, and 337, 1996.
18. K. S. Suslick, Sonochemistry of Transition Metal Compounds, in R. B. King (ed.), *Encyclopedia of Inorganic Chemistry;* New York: Wiley, vol. 7, pp. 3890–3905.
19. Lord Rayleigh, On the pressure developed in a liquid during the collapse of a spherical cavity, *Philos. Mag.,* **34**: 94, 1917.
20. W. T. Richards and A. L. Loomis, The chemical effects of high frequency sound waves: I. A preliminary study, *J. Amer. Chem. Soc.,* **49**: 3086, 1927.

21. B. P. Barber and S. J. Putterman, Light-scattering measurements of the repetitive supersonic implosion of a sonoluminescence bubble, *Phys. Rev. Lett.,* **69**: 3839, 1992.
22. R. Lofstedt, B. P. Barber, and S. J. Putterman, Toward a hydrodynamic theory of sonoluminescence, *Phys. Fluids* **A 5**: 2911, 1993.
23. A. Henglein, Contributions to various aspects of cavitation chemistry, *Adv. Sonochem.,* **3**: 17, 1993.
24. H. Frenzel and H. Schultes, Luminescenz im ultrashallbeschickten wasser, *Z. Phys. Chem.* **27b**: 421, 1934.
25. T. J. Matula et al., Comparison of single-bubble and multi-bubble sonoluminescence spectra, *Phys. Rev. Lett.,* **75**: 2602, 1995.
26. D. F. Gaitan and L. A. Crum, Observation of Sonoluminescence from a Single, Stable Cavitation Bubble in a Water/Glycerine Mixture, in M. Hamilton and D. T. Blackstock (eds.), *Frontiers of Nonlinear Acoustics,* 12th ISNA, New York: Elsevier Appl. Sci., 1990, pp. 459–463.
27. D. F. Gaitan et al., Sonoluminescence and bubble dynamics for a single, stable cavitation bubble, *J. Acoust. Soc. Amer.,* **91**: 3166, 1992.
28. L. A. Crum and R. A. Roy, Sonoluminescence, *Science,* **266**: 233, 1994.
29. B. P. Barber et al., Defining the unknowns of sonoluminescence, *Phys. Rep.,* **281**: 66–143, 1997.
30. Y. T. Didenko, Water sonoluminescence spectra produced by CW and pulsed ultrasound, *Acous. Phys.,* **43**: 215, 1997.
31. E. B. Flint and K. S. Suslick, Sonoluminescence from alkali–metal salt solutions, *J. Phys. Chem.,* **95**: 1484, 1991.
32. E. B. Flint and K. S. Suslick, Sonoluminescence from nonaqueous liquids: Emission from small molecules, *J. Amer. Chem. Soc.,* **111**: 6987, 1989.
33. V. Kamath, A. Prosperetti, and F. N. Egolfopoulos, A theoretical study of sonoluminescence, *J. Acoust. Soc. Amer.,* **94**: 248, 1993.
34. B. Gompf et al., Resolving sonoluminescence pulse width with time-correlated single-photon counting, *Phys. Rev. Lett.,* **79**: 1405, 1997.
35. B. P. Barber et al., Resolving the picosecond characteristics of synchronous sonoluminescence, *J. Acoust. Soc. Amer.,* **91**: 3061, 1992.
36. B. P. Barber and S. J. Putterman, Observation of synchronous picosecond sonoluminescence, *Nature,* **352**: 318, 1991.
37. T. J. Matula, R. A. Roy, and P. D. Mourad, Optical pulse width measurements of sonoluminescence in cavitation-bubble fields, *J. Acoust. Soc. Amer.,* **101**: 1994, 1997.
38. D. Lohse et al., Sonoluminescing air bubbles rectify argon, *Phys. Rev. Lett.,* **78**: 1359, 1997.
39. D. Lohse and S. Hilgenfeldt, Inert gas accumulation in sonoluminescing bubbles, *J. Chem. Phys.,* **107**: 6986–6997, 1997.
40. J. Matula and L. A. Crum, Evidence for gas eschange in single-bubble sonoluminescence, *Phys. Rev. Lett.,* **80**: 865–868, 1998.
41. K. R. Weninger, B. P. Barber, and S. J. Putterman, Pulsed miescattering measurements of the collapse of a sonoluminescing bubble, *Phys. Rev. Lett.,* **78**: 1799, 1997.
42. W. C. Moss et al., Calculated pulse widths and spectra of a single sonoluminescing bubble, *Science,* **276**: 1398, 1997.
43. K. R. Weninger, S. J. Putterman, and B. P. Barber, Angular correlations in sonoluminescence: Diagnostic for the sphericity of a collapsing bubble, *Phys. Rev.,* **A 54**: R2205–R2208, 1996.
44. T. J. Mason and E. D. Cordemans, Ultrasonic intensification of chemical processing and related operations—A review, *Chem. Eng. Res. Des.,* **74**: 511, 1996.
45. R. L. Hunicke, Industrial applications of high power ultrasound for chemical reactions, *Ultrasonics,* **28**: 291, 1990.
46. P. Riesz, Free radical generation by ultrasound in aqueous solutions of volatile and non-volatile solutes, *Adv. Sonochem.,* **2**: 23, 1991.
47. V. Misik and P. Riesz, Recent applications of epr and spin trapping to sonochemical studies of organic liquids and aqueous solutions, *Ultrason. Sonochem.,* **3**: S173, 1996.
48. M. A. Margulis and N. A. Maximenko, Influence of ultrasound on oscillating reactions, *Adv. Sonochem.,* **2**: 253, 1991.
49. I. Hua, R. H. Hochemer, and M. R. Hoffmann, Sonochemical degradation of P-nitrophenol in a parallel-plate near-field acoustic processor, *Env. Sci. Tech.,* **29**: 2790, 1995.
50. C. Petrier and S. Laguian, Ultrasonic degradation at 20 Khz and 500 Khz of atrazine and pentachlorophenol in aqueous solution-preliminary results, *Chemosphere,* **32**: 1709, 1996.
51. K. S. Suslick et al., Alkane sonochemistry, *J. Phys. Chem.,* **87**: 2229, 1983.
52. K. S. Suslick, Organometallic sonochemistry, *Adv. Organomet. Chem.,* **25**: 73, 1986.
53. O. V. Abramov, *Ultrasound in Liquid and Solid Metals,* Boca Raton, FL: CRC Press, 1994.
54. K. S. Suslick et al., Sonochemical synthesis of amorphous iron, *Nature,* **353**: 414, 1991.
55. M. W. Grinstaff, M. B. Salamon, and K. S. Suslick, Magnetic properties of amorphous iron, *Phys. Rev.,* **B 48**: 269, 1993.
56. T. Hyeon, M. Fang, and K. S. Suslick, Nanostructured molybdenum carbide: sonochemical synthesis and catalytic properties, *J. Amer. Chem. Soc.,* **118**: 5492, 1996.
57. K. S. Suslick, M. Fang, and T. Hyeon, Sonochemical synthesis of iron colloids, *J. Amer. Chem. Soc.,* **118**: 11960, 1996.
58. K. S. Suslick, Sonocatalysis, in G. Ertl, H. Knozinger, and J. Weitkamp (eds.), *Handbook of Heterogeneous Catalysis.* Weinheim: Wiley-VCH: 1997; vol. 3, ch. 8.6, pp. 1350–1357.
59. K. S. Suslick and M. W. Grinstaff, Protein microencapsulation of nonaqueous liquids, *J. Amer. Chem. Soc.,* **112**: 7807, 1990.
60. K. J. Liu et al., In vivo measurement of oxygen concentration using sonochemically synthesized microspheres, *Biophys. J.,* **67**: 896, 1994.
61. T. Ando and T. Kimura, Ultrasonic organic synthesis involving non-metal solids, *Adv. Sonochem.,* **2**: 211, 1991.
62. A. Durant et al., Sonoelectrochemistry—the effects of ultrasound on organic electrochemical reduction, *Electrochim. Acta,* **41**: 277, 1996.
63. R. G. Compton, J. C. Eklund, and F. Marken, Sonoelectrochemical processes—A review, *Electroanalysis,* **9**: 509, 1997.
64. J. L. Anderson, L. A. Coury, and J. Leddy, Dynamic electrochemistry—methodology and application, *Analytical Chem.,* **70**: R519–R589, 1998.
65. A. Durant et al., A new procedure for the production of highly reactive metal powders by pulsed sonoelectrochemical reduction, *Tetrahedron Lett.,* **36**: 4257, 1995.

KENNETH S. SUSLICK
University of Illinois at Urbana–Champaign
THOMAS J. MATULA
University of Washington

ULTRASONIC PROCESSING. See HIGH POWER ULTRASOUND.

ULTRASONICS. See GEOPHYSICAL PROSPECTING USING SONICS AND ULTRASONICS; PHYSICAL ACOUSTICS.